Kinetics of Charge Separation in Poly(A)−Poly(T) DNA Hairpins

Gail S. Blaustein,[†] Frederick D. Lewis,[‡] and Alexander L. Burin*[,†]

Department of Chemistry, Tulane University, New Orleans, Louisiana 70118, and Department of Northwestern University, Evanston, Illinois 60208

Received: February 11, 2010; Revised Manuscript Received: April 9, 2010

A kinetics model is designed to investigate the charge separation (CT) process in stilbene-capped DNA hairpins composed of AT base pairs. This model combines standard tunneling and hopping electron transport with exciplex formation upon photoexcitation of the acceptor stilbene and its neighboring adenine and is capable of interpreting the CT rate and yield data within experimental accuracy. An analysis of hopping transport within the framework of a 1-D diffusion model results in a calculation of the nearest-neighbor CT rate to be approximately 1.2 ns^{-1}. In agreement with previous experimental and theoretical work, it is ascertained through a novel application of an extension to classical Marcus theory that the nearest-neighbor CT is adiabatic with reorganization energy $\lambda \sim 0.83$ eV. The kinetics model can be extended to accurately characterize CT in other poly(A)−poly(T) systems with different hole donors (naphthaldiimide and 2-aminopurine) and acceptors (phenothiazine and guanine).

I. Introduction

Although the ability of DNA to conduct charge has been discussed for over 50 years,[1,2] the mechanism continues to be a topic of great scientific interest and debate.[3] The phenomenon of charge transfer in DNA is of fundamental interest because it presents a unique juxtaposition of strongly coupled electron quantum dynamics with the classical mechanical behavior of water, a highly polar solvent. In addition, charge transfer stimulated by DNA photoexcitation and photoionization leads to biologically significant radiative damage[4] and can be an important factor in enzyme functionality for living organisms.[5] The natural availability of DNA together with its potential to conduct charge lends itself to possible applications in nanotechnology including molecular electronics[6−9] and solar energetics.[10] These fundamental and practical motivations have stimulated a growing number of experimental and theoretical studies; however, the charge quantum state in DNA and the particular mechanisms controlling charge transfer remain subjects of controversy due to the convoluted nature of existing experimental data and the tremendous complexity of the system itself.[6,11−24]

The main goal of the present work is to interpret experimental data that are associated with the charge separation process in DNA hairpins with AT bridges of various lengths. Experimental data for time-resolved measurements of charge transfer (CT) in DNA have been published extensively for a variety of nucleobase sequences and segment lengths. For instance, very recent work by Lewis and co-workers includes charge separation studies of stilbene-capped hairpins containing sequences of AT and GC pairs[25,26] (see also the theoretical analysis of Grozema et al.[27]). Another investigation of charge transfer in DNA by Majima and co-workers involves the substitution of adenine with 7-deazaadenine.[28] In contrast, our focus is on a relatively simple sequence of AT pairs because our successful characterization of this system will provide a strong foundation for modeling more complicated ones.

Mixed sequences are inherently more difficult to characterize due to the varied ionization potentials of the nucleobases in the path of the migrating charge. In addition, it is observed that CT in mixed sequences has reduced efficiency and in some cases can actually be suppressed if the charge is trapped at a nucleobase with a lower ionization potential than that in its vicinity.[29−33] The most efficient charge transfer is expected to be in sequences of (nonalternating) identical base pairs that are characterized by the nearest-neighbor CT rate k.

In this work, we derive a kinetics model for charge separation in stilbene-capped DNA hairpins, which includes both charge hopping and tunneling channels and provides a robust interpretation of experimental data within experimental accuracy. We use this model to determine the CT rate k, and by a novel application of Rips and Jortner's extension to Marcus theory,[34] we calculate the reorganization energy λ and show that nearest-neighbor CT is an adiabatic process. In addition, we detail the application of this kinetics model to the poly(A)−poly(T) systems of Wan et al. and Takada et al.[12,14] and show that data fitting within experimental accuracy can be achieved for these systems as well.

II. Analysis of Charge Separation Experimental Data

Experimental Data. In this section, we develop our charge separation kinetics model based on experimental data for stilbene-capped DNA hairpins with poly-A−poly-T sequences of the form $(AT)_n$, $n = 1, ..., 7$ (see Table 1 and the work of Lewis et al.[10]). Stilbenediamide (Sa) and stilbenediether (Sd) capped DNA hairpins as shown in Figure 1, where Sa and Sd label the electron acceptor and donor stilbene, respectively, provide useful quantitative data. The photoexcitation of Sa can result in a charge separation reaction oxidizing either the bridge or Sd or both in succession. Transient absorption measurements are used to study the formation and decay of $Sa^{-\bullet}$ and $Sd^{+\bullet}$ states as well as charge transfer kinetics. Only $Sa^{-\bullet}$ contributes to the transient absorption band at 575 nm, whereas both $Sa^{-\bullet}$ and $Sd^{+\bullet}$ contribute to the 525 nm absorption band. An analysis

* Corresponding author. E-mail: aburin@tulane.edu.
[†] Tulane University.
[‡] Northwestern University.

10.1021/jp101328t © 2010 American Chemical Society
Published on Web 04/27/2010

TABLE 1: Summary of Experimental Data (exp.) Compared to Calculations Using Our Theoretical Model (th.) for Charge Separation Yield Φ_s and Hole Arrival Time τ_s (ps) for a Family of AT_n Bridges

n	1	2	3	4	5	6	7
Φ_s, exp.	1	0.8 ± 0.2	0.52 ± 0.08	0.23 ± 0.01	0.10 ± 0.05	0.09 ± 0.03	0.06 ± 0.03
Φ_s, th.	0.99	0.93	0.61	0.22	0.10	0.079	0.071
τ_s, exp.	5 ± 1	49 ± 3	250 ± 30	1300 ± 300	4500 ± 2000	9000 ± 4000	12000 ± 4000
τ_s, th.	5.6	44	250	1300	5300	8500	11000
τ_t	5.6	43	220	440	490	500	500
τ_h	520	1300	2500	4200	6200	8600	11000
Y_t	1.0	0.99	0.92	0.62	0.18	0.03	0.004
Y_h	0.002	0.01	0.08	0.38	0.82	0.97	1.0

of the time-dependent ratio of the two band intensities permits determination of two important characteristics of charge transfer: (a) the charge separation quantum yield or the probability of the $Sa^{-\bullet}(AT)_nSd^{+\bullet}$ state formation, and (b) the approximate time of the formation of $Sd^{+\bullet}$, also called the hole arrival time.[10] The bridge length dependent quantum yield and hole arrival time contain important information about the nature of charge transport within a DNA bridge.

Our analysis of experimental data is based on a kinetics model schematically depicted in Figure 2. Time-resolved measurements show that a large percentage of hairpins in the photoexited state Sa* undergo conversion to short-lived excited species during the first 30 ps of measurements as indicated by the transient absorption spectrum and fast fluorescence decay. However, it

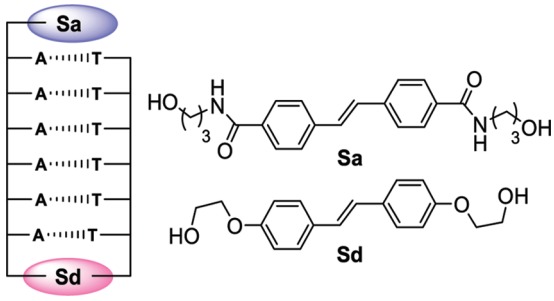

Figure 1. Schematic of a poly-A−poly-T DNA hairpin capped by a stilbene acceptor (Sa) and a stilbene donor (Sd) group.

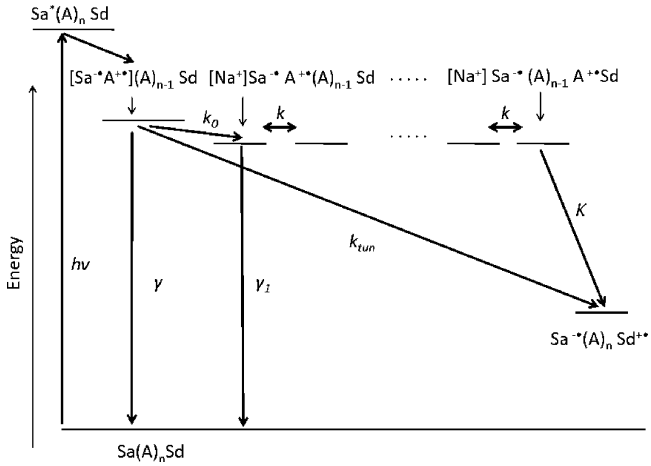

Figure 2. Mechanisms of charge separation. First, the photoexcited state $Sa^*(A)_nSd$ is formed after absorption of a photon with energy $h\nu$. Then this state rapidly decays, forming exciplex $[Sa^{-\bullet}\ A^{+\bullet}]\ A_{n-1}Sd$ during the first 30 ps. The exciplex decays due to hole tunneling to Sd (rate k_{tun}), charge recombination (rate γ), or stabilization of the $Sa^{-\bullet}A^{+\bullet}(A)_{n-1}Sd$ state are possibly due to counterion Na^+ attachment to $Sa^{-\bullet}$ (rate k_0). k is the charge hopping rate on the AT bridge, and the final irreversible step of charge transfer proceeds with rate K forming the $Sd^{+\bullet}$ radicalized cation.

is suggested by Lewis et al.[35] that the conversion is actually much faster, perhaps as fast as 2 ps, and that band shape changes can be attributed to the reversible formation of a mixture of the exciplex state $[Sa^{-\bullet}A^{+\bullet}](A)_{n-1}Sd$ and singlet state $Sa^*(A)_nSd$ which favors the exciplex. Using the fluorescence decay components (ca. 30% long-lived) and fluorescence quantum yield (ca. 0.3), a yield of ca. 10% $Sa^*(A)_nSd$ and 90% $[Sa^{-\bullet}A^{+\bullet}](A)_{n-1}Sd$ can be estimated.

The exciplex state $[Sa^{-\bullet}(A)^{+\bullet}](A)_{n-1}Sd$ decays to the charge separated state $Sa^{-\bullet}(A)_nSd^{+\bullet}$ via two possible channels: direct hole tunneling through the AT bridge to Sd and hole hopping along the AT bridge. The tunneling process is characterized by the rate k_{tun}, which decreases exponentially with bridge length. The more involved hopping process begins with the decay of the exciplex $[Sa^{-\bullet}A^{+\bullet}](A)_{n-1}Sd$ to a state that allows the release of the hole onto the bridge, with rate k_0. We propose that the Na^+ counterion present in solution influences this rate by screening the Coulomb attraction between the two ions in $[Sa^{-\bullet}A^{+\bullet}]$ (see Section IV). Although this counterion activity is not involved with the actual hopping kinetics, we include $[Na^+]$ in Figure 2 to acknowledge its influence on the exciplex. This interaction of the hairpin with Na^+ allows the hole to hop between adjacent A bases with rate k. When the hole reaches the nth adenine, it migrates directly to Sd with rate K. Charge recombination channels from the exciplex state $[Sa^{-\bullet}A^{+\bullet}](A)_{n-1}Sd$ with rate γ and from the oxidized state $[Na^+]Sa^{-\bullet}A^{+\bullet}(A)_{n-1}Sd$ with rate γ_1 are also included since they play an important role in both the time-dependent kinetics and quantum yield of charge separation. We ignore oxidation of T due to its higher ionization potential than A.

In our model, we assume that $K \gg k$ since Sd has a lower ionization potential than A resulting in a large driving force behind CT from the nth A to Sd.[10] This assumption allows for an excellent fit with the experimental data for both charge separation yield and hole arrival time (see Table 1 and Figure 3).

Kinetics Model. Considering the short time required for the formation of the exciplex (ca. 2 ps) and the longer times required for hole tunneling to Sd (Table 1), we can for all practical purposes consider the exciplex as the initial state at time $t = 0$. This assumption is well justified for long sequences ($n \geq 4$) where the nearest-neighbor CT mechanism is dominated by DNA hole transport dynamics and independent of the specific mechanisms of hole creation and injection.

Let P_{exc}, P_1, P_2, ..., P_n, and P_{Sd} represent the probabilities of finding a hole at the exciplex $[Sa^{-\bullet}A^{+\bullet}]$, A_i ($i = 1, ..., n$), and Sd, respectively, at time t. For time $t = 0$, we have the following initial conditions: $P_{exc} = 1$, $P_1 = ... = P_n = P_{Sd} = 0$. As the rate of charge recombination from the $Sa^{-\bullet}(AT)_nSd^{+\bullet}$ (charge separated) state to the ground state is shown experimentally to be several orders of magnitude slower than charge separation,[10]

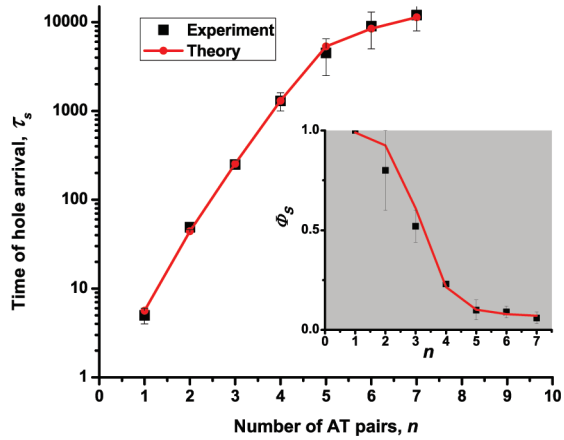

Figure 3. Comparison of experimental data[10] with theory for hole arrival time and charge separation yield (inset).

the charge separated state can reasonably be considered an end state in our charge separation kinetics model.

Then, according to Figure 2, we have the following set of rate equations

$$\begin{aligned}
\frac{dP_{\mathrm{exc}}}{dt} &= -(\gamma + k_0 + k_{\mathrm{tun}})P_{\mathrm{Sa}} \\
\frac{dP_1}{dt} &= k_0 P_{\mathrm{Sa}} + kP_2 - (k + \gamma_1)P_1 \\
\frac{dP_i}{dt} &= k(P_{i-1} + P_{i+1}) - 2kP_i,\ 1 < i < n \\
\frac{dP_n}{dt} &= kP_{n-1} - (k + K)P_n \\
\frac{dP_{\mathrm{Sd}}}{dt} &= KP_n + k_{\mathrm{tun}}P_{\mathrm{Sa}}
\end{aligned} \tag{1}$$

In our model, we assume that nearest-neighbor CT (hopping) on the homogeneous AT bridge is unbiased. The only possible source of bias is the Coulomb attractive force of the unscreened $Sa^{-\bullet}$ ion. As stated above, we assume that the hole cannot hop on the AT bridge unless the Na^+ counterion screens the attractive force between $Sa^{-\bullet}$ and the adjacent $A^{+\bullet}$, thus significantly lessening this bias. In light of this condition, we believe that the bias, if it exists, is too small to influence the kinetics of nearest-neighbor CT. As will be seen in Section III, this assumption is well-supported by the excellent agreement between our results and the experimental data.

The values of interest to be calculated using our model are the charge separation yield Φ_s and the hole arrival time τ_s. The charge separation yield can be defined as $\Phi_s = P_{\mathrm{Sd}}(t \to \infty)$ or the probability of occupation of the Sd site by the hole in the asymptotic limit. This value can be calculated analytically using the Laplace method. The hole arrival time τ_s is calculated using the numerical solution for the time-dependent probability of the hole arrival $P_{\mathrm{Sd}}(t)$.

The result for the yield in the limit of the charge transfer rate $K \gg k$ can be expressed as

$$\begin{aligned}
\Phi_s &= \Phi_t + \Phi_h, \text{ with} \\
\Phi_t &= \frac{k_{\mathrm{tun}}}{k_{\mathrm{tun}} + \gamma + k_0} \\
\Phi_h &= \frac{k_0}{k_{\mathrm{tun}} + \gamma + k_0} \cdot \frac{k}{k + \gamma_1(n-1)}
\end{aligned} \tag{2}$$

The first term Φ_t is responsible for the tunneling contribution, while the second term Φ_h is responsible for the hopping contribution. The relative yields Y_t and Y_h due to tunneling and hopping, respectively, are given by

$$Y_t = \frac{\Phi_t}{\Phi_s} \text{ and } Y_h = \frac{\Phi_h}{\Phi_s} \tag{3}$$

In accordance with the experimental method of performing an exponential data fit,[10] we determined the hole arrival time by considering the solution

$$P_{\mathrm{Sd}}(t) = \Phi_s(1 - e^{-t/\tau_s}) \tag{4}$$

with initial and final conditions $P_{\mathrm{Sd}}(t) = 0$ and $P_{\mathrm{Sd}}(\infty) = \Phi_s$ respectively. Then, for arrival time τ_s, we have

$$P_{\mathrm{Sd}}(\tau_s) = \Phi_s(1 - e^{-1}) \tag{5}$$

The characteristic arrival time τ_s has been determined by solving eq 1 numerically. We also calculated partial arrival times τ_t and τ_h which are the arrival times for the tunneling and hopping processes, respectively. τ_t and τ_h are determined by setting $k = 0$ and $k_{\mathrm{tun}} = 0$, respectively, in eq 2. The analytical expression for the hole arrival time for the tunneling mechanism is simply

$$\tau_t = \frac{1}{k_{\mathrm{tun}} + \gamma + k_0} \tag{6}$$

However, we were not able to obtain a similar compact analytical expression for τ_h.

III. Results

Kinetic Analysis. The analytical solution to eq 2 and the numerical solution to eq 5 were compared to experimental data as shown in Table 1 and Figure 3. Fitting parameters for all rates were determined by the least-squares method for all experimental data in Table 1 with respect to their theoretical expectations. The average deviation of theoretical values from experimental values is less than 10%, which is comparable to experimental accuracy. We also show partial arrival times for tunneling and hopping channels and relative yields for both channels calculated in accordance with eqs 2 and 3.

Let us briefly discuss each fitting parameter. The tunneling rate $k_{\mathrm{tun}}(r) = K_0 \exp(-\beta r)$, where $r = n(3.4\ \text{Å})$ is the bridge length, has a preexponential factor $K_0 = 12\ \mathrm{ps}^{-1}$, which is quite reasonable for charge transfer with a large driving force to the charge separated state $Sd^{+\bullet}$. The parameter $\beta = \ln(8.3)/3.4 \approx 0.62\ \text{Å}^{-1}$ is typical for distance-dependent charge transfer between DNA bases separated by an AT bridge.[31] The recombination rate $\gamma = 1.7 \times 10^{-3}\ \mathrm{ps}^{-1}$ is close to the decay rate for the slow fluorescence component discussed in Section III. The

rate of "hole release" $k_0 = 0.22 \times 10^{-3}$ ps^{-1} from Sa to its neighboring A can be justified by the slow Na^+ counterion diffusion rate (see next section) in agreement with the qualitative estimates of our earlier work.[36] If our expectations are correct, then the rate k_0 can be altered by counterion substitution. The recombination rate $\gamma_1 = 0.29 \times 10^{-3}$ ps^{-1} for the hole located at the A base adjacent to Sa is much slower than the recombination rate for an adjacent oxidized guanine most likely because the relaxation of $Sa^{-\bullet}G^{+\bullet}\cdots Sd$ to the ground state has a greater driving force in the inverted Marcus regime.[37,38] The charge hopping rate between adjacent A bases is found to be $k = 1.2 \times 10^{-3}$ ps^{-1}, which is perhaps the most interesting result derived from our analysis.

In our model, we find that the tunneling mechanism is mostly responsible for charge separation in DNA hairpins with $n < 4$ AT pairs, while for $n > 4$ the hopping mechanism dominates. However, for $n = 4$, we observe that both channels contribute significantly and almost equally to the rate (62% tunneling and 38% hopping).

It is interesting to note that the experimentally determined hole arrival time in the tunneling regime τ_t is not purely the inverse of tunneling rate k_{tun} but is instead determined by the inverse of the combined decay rate $(k_{tun} + \gamma + k_0)^{-1}$ (see eq 6 and Table 1). However, this is not the case for the hopping transport, where the arrival time $\tau_h \sim n^2/k$ is only weakly sensitive to the competing recombination rate γ_1, the reason being that successful charge separation events are determined by random walks that rarely take the charge back to the first AT base pair where recombination can occur. For large bridge lengths n, the likelihood of a random walk taking the hole back to the first AT base pair decreases with $1/n$ as reflected by the yield behavior (eq 2). Thus, our model is sufficient for the calculation of charge separation times in the hopping regime, and we indeed find the dependence $\tau_s \propto n^2$ in measurements at longer bridge lengths (see Section IV).

Reorganization Energies. There have been many important contributions[39−42,34] to further the generalization and applicability of classical Marcus Theory[43−45] in both the nonadiabatic and adiabatic regimes. The following is based on the general analysis of a CT problem by Rips and Jortner.[34]

To obtain the general characterization of a CT process as either nonadiabatic or solvent-controlled adiabatic, we apply the adiabaticity parameter

$$\kappa_A = \frac{4\pi b^2 \tau_L}{\hbar\lambda} \tag{7}$$

where b, τ_L, and λ represent the electron overlap integral (or electronic coupling), the longitudinal dielectric relaxation time of the solvent, and the reorganization energy. For $\kappa_A \ll 1$, the process is nonadiabatic, and for $\kappa_A \gg 1$, the process is considered solvent-controlled adiabatic.

Consider Rips and Jortner's Arrhenius-based rate equation

$$k = A \exp\left(-\frac{(\Delta G^\circ + \lambda)^2}{4\lambda k_B T}\right) \tag{8}$$

where the preexponential factor is given as

$$A_{NA} = \frac{2\pi b^2}{\hbar\sqrt{4\pi\lambda k_B T}} \tag{9}$$

for the nonadiabatic process and

$$A_A = \tau_L^{-1}\sqrt{\frac{\lambda}{16\pi k_B T}} \tag{10}$$

for the solvent-controlled adiabatic process. Since CT occurs between two adenine nucleobases, the free energy $\Delta G^\circ = 0$.[46] Hence, eq 8 reduces to

$$k = A \exp\left(-\frac{\lambda}{4k_B T}\right) \tag{11}$$

We can find the reorganization energy λ at high temperature ($T = 300$ K) when we take $\tau_L = 0.21$ ps for water ($\tau_L = (\varepsilon_\infty/\varepsilon_S)\tau_D$[34] with $\varepsilon_\infty = 1.8$, $\varepsilon_S = 80$, and $\tau_D = 9.36 \times 10^{-12}$ s) and $b = 0.10$ eV, a reasonable value for nearest-neighbor CT.[47,48] However, Blancafort and Voityuk have found that $b \sim 0.070$ eV using the CAS method.[49] This result is still a rough approximation since b strongly depends on the influence of neighboring base pairs and fluctuates by several orders of magnitude with intrabase pair deformations.[50−52]

The application of eq 11 for the nonadiabatic limit yields

$$\lambda_{NA} = 1.2 \text{ eV} \tag{12}$$

and for the adiabatic limit

$$\lambda_A = 0.83 \text{ eV} \tag{13}$$

When $\lambda_{NA} = 1.2$ eV and $\lambda_A = 0.83$ eV are applied to eq 7, $\kappa_A = 33$ and 48, respectively, with both satisfying the condition $\kappa_A \gg 1$ for a process in the solvent-controlled adiabatic regime. To further support this result, we find that the preexponential factor for the rate equation in the adiabatic regime is smaller than that in the nonadiabatic regime since CT is controlled by the rate-limiting process.[34] Indeed, for $\lambda = 0.83$ eV, we have $A_{NA} = 180$ ps^{-1} and $A_A = 3.5$ ps^{-1}, and from eq 7, we have adiabaticity parameter $\kappa_A = A_{NA}/A_A \approx 51 \gg 1$. Since the adiabatic preexponential factor A_A does not depend on b, intramolecular deformation is not a factor in our kinetics model.

Nevertheless, $b \sim 0.1$ eV is an appropriate choice for our calculations. Indeed, following eq 7 and the criterion for adiabatic CT,[34] charge transfer is an adiabatic process for

$$b > \sqrt{\frac{\hbar\lambda}{4\pi\tau_L}} \tag{14}$$

with $b > 0.014$ eV using $\lambda = 0.83$. According to Rips and Jortner, eq 14 also agrees with the Landau−Zener criterion for adiabatic to nonadiabatic transition.[34,53] Furthermore, for $b \sim k_B T$, adiabatic transition can also occur through the first excited state.

The total reorganization energy λ for charge transfer in DNA is defined by

$$\lambda = \lambda_s + \lambda_i \tag{15}$$

where λ_s and λ_i are the solvent reorganization energy and the internal (molecular) reorganization energy contributions,

respectively.[54,55] Both contributions are important in our estimate of the adiabatic reorganization energy (eq 13); however, λ_s is larger than λ_i.[55]

The use of the water relaxation time τ_s (not to be confused with the charge separation time used in the context of our kinetics model) in the preexponential factor eq 10 is approximate because the internal relaxation time τ_i may be different. The correct expression for the average relaxation time is[34]

$$\tau_L^{-1} = \frac{\lambda_s/\tau_s + \lambda_i/\tau_i}{\lambda_i + \lambda_s} \tag{16}$$

We believe that the difference between using τ_s or τ_L from eq 16 is negligible for our estimate since the reorganization energy is only logarithmically related to the relaxation time.

IV. Discussion

Charge Separation in DNA Hairpins. As mentioned above in Section II, both fluorescence decay and transient absorption experimental data[35] show that charge separation occurs within 30 ps of the photoexcitation of Sa in the formation of the exciplex state $[Sa^{-\bullet}A^{+\bullet}](A)_{n-1}Sd$. Since approximately 30% of fluorescence decays more slowly with a fluorescence quantum yield of ca. 0.3, this indicates that about 10% of photoexcited hairpins remain in the $Sa^*(A)_nSd$ state. Meanwhile, for approximately 90% of the population, the fluorescence decay rate is indicative of charge movement and the formation of the exciplex state $[Sa^{-\bullet}A^{+\bullet}](A)_{n-1}Sd$.

The exciplex decays via three possible channels: hole tunneling to Sd, radiative and nonradiative relaxation to the ground state, and the formation of the state $[Na^+]Sa^{-\bullet}A^{+\bullet}(A)_{n-1}Sd$ capable of releasing the hole to hop along the DNA bridge. Its estimated recombination rate or rate of relaxation $\gamma \sim 1.7 \times 10^{-3}$ ps^{-1} agrees with the observed fluorescence slow decay rate.[10] Tunneling of the hole from the exciplex to Sd may occur for short sequences with $n < 4$, which is consistent with our kinetics model. However, for the sequence containing only one AT pair ($n = 1$), the structure of the hairpin can also deviate from the equilibrium structure, and then the relevance of our model for that sequence may be a random coincidence. For $n > 1$, the hole is prevented from hopping to the second A because of its strong Coulomb attraction to the $Sa^{-\bullet}$ ion while located at the first A. According to the work of Grozema et al., this interaction results in a potential barrier as high as 0.5−1 eV for the hole to migrate to the second A.[24]

Overcoming the potential barrier for charge separation requires a significant external influence. Grozema et al. attribute hole migration to structural fluctuations which increase electronic coupling between adjacent A bases. In addition, the effect on the rate k_0 by the interaction between the Na^+ counterion and $Sa^{-\bullet}$ can possibly influence charge separation via hole migration. This counterion effect on the rate is analogous to that of Cl^- attachment which we propose is responsible for the dual-exponential kinetics of charge recombination in the same family of hairpins.[36] Counterion attachment (not necessarily by means of chemical bonding) leads to a decrease in the Coulombic attractive force between the hole and $Sa^{-\bullet}$, thus freeing it to hop through the bridge.

Another, and in our opinion, less probable scenario regarding the influence of the Na^+ counterion on CT involves ion-gated transport phenomena[56] where the charge neutralizing effect of Na^+ counterions along the negatively charged phosphate backbone inhibit the migration of the hole to the second A. Once the counterion at the backbone near the second A moves away, the hole can migrate to the second A due to electrostatic attractive forces.

Our expectations regarding the influence of counterions on CT are consistent with molecular dynamics-based analysis by Kubar and Elstner.[57] They found that the counterions represent a component of a system that has a major impact on CT energetics. Counterions and water interact collectively with DNA, producing a strong screening effect enabling hole migration.

The reorganization energy $\lambda = 0.83$ eV is in agreement with the experimentally derived $\lambda = 0.92 \pm 0.45$ eV of Lewis et al.[58] However, theoretical studies[59,60] yielded total reorganization energies of higher values overall due to the computational methods employed.[61] Although quantum mechanical methods are used to calculate internal reorganization energy λ_i and generally agree with experimental results,[58,62] the discrepancy can be attributed to the use of classical methods for determining the solvent reorganization energy λ_s. For instance, in the case of Siriwong et al., the overestimation of λ_s is attributed to the choice of dielectric constant assigned to the DNA base stack zone.[55] In another example, Kubar and Elstner found $\lambda_s = 1.21$ eV for A to A CT using MM force field calculations,[61] while Steinbrecher et al. documented $\lambda_s = 1.08$ eV.[48] MM calculations account classically for all vibrational energies; however, this method does not work well for the high-frequency ground-state vibrations of H−, C−C, or C−N bonds, thus leading to overestimations.

Accounting for quantum mechanical delocalization of charge can reduce computationally derived reorganization energy values.[50] Delocalization is determined by the relationship between the reorganization energy and the electron transfer integral b.[23] Since particularly in our case, $b \ll \lambda$, where we have $b \sim 0.05-0.1$ eV and $\lambda \sim 0.8$ eV, the delocalization is expected to be very weak.

In Section II, we assumed that the charge hopping toward the AT bridge is unbiased despite possible Coulomb attraction between $Sa^{-\bullet}$ and $AT^{+\bullet}$. To quantitatively verify whether this assumption is reasonable, we also attempted to fit experimental data for stilbene-capped hairpins using an alternative kinetics model where nearest-neighbor CT is affected by this Coulomb attraction. The Coulomb attraction for the nth base pair is defined by

$$U(n) \approx -U_c/n \tag{17}$$

where U_c is an adjustable parameter. Then, the nearest-neighbor CT rates can be expressed as

$$k_{n,n-1} = k \exp\left(\frac{-(U(n) - U(n-1))}{k_B T}\right)$$
$$k_{n-1,n} = k \exp\left(\frac{U(n) - U(n-1))}{k_B T}\right) \tag{18}$$

from the $(n-1)$th base pair to the nth base pair and backward, respectively. The charge migration rate was chosen to be $k \approx 10$ ns^{-1}.[13] Under these assumptions, a reasonable data fit is possible if one chooses $U_c \approx 0.05$ eV, a factor of 30 smaller than the estimate of Grozema et al.[24] This choice is clear because the Coulomb attraction reduces the hopping transport rate by a factor of $\exp(-U_c/k_BT)$, and a larger Coulomb attraction will make hopping inefficient due to its exponential suppression. However, we do not think that the Coulomb interaction is

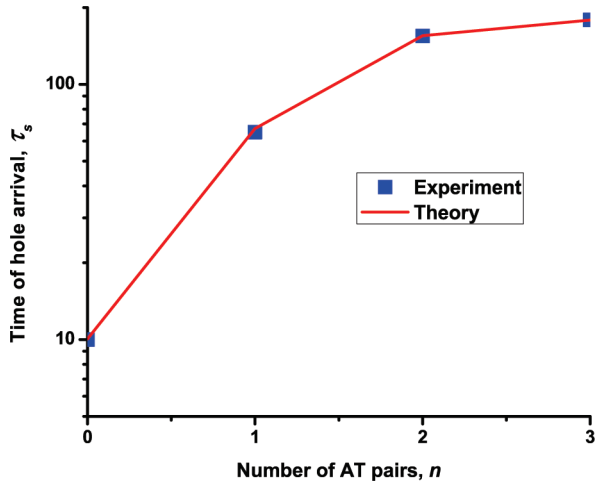

Figure 4. Comparison of experimental data[12] with theory for hole arrival time at G from AP* depending on the number n of AT pairs separating them.

overestimated by Grozema et al. by almost 2 orders of magnitude. Therefore, we believe that only the screening of the Coulomb interaction by counterions can be responsible for an almost unbiased nearest-neighbor CT.

Application of the Kinetics Model to Other Systems. To further validate our kinetics model, we examined its applicability to other poly(A)−poly(T) hairpin systems. Data fitting has been successfully performed within experimental error to systems described in the published work of Wan et al. and Takada et al.[12,14]

Changes in the AP decay times were obtained by Wan et al. for hairpins consisting of photoexcited 2-aminopurine (AP) and guanine (G) separated by an $(AT)_n$ bridge with $n = 0, ..., 3$. By assuming that these changes were the result of differences in CT rates, they were able to deduce the CT arrival times to be 10, 65, 155, and 179 ps for $n = 0, ..., 3$, respectively.[12,63] Using the assumption from our analysis above that quantum tunneling is the CT mechanism for $n < 4$, we can characterize the CT rate as

$$k_{tun,ap}(r) = k_{ap} \exp(-\beta_{ap} r) \tag{19}$$

where r is the distance between AP and G; k_{ap} is the rate constant; and β is the distance range parameter. We convert $k_{tun,ap}(r)$ to $k_{tun,ap}(n)$ by setting $r = 3.4(n + 1)$ Å. Taking into account that AP* does not oxidize the adjacent A, but tunnels directly to G, we modified eq 6 so that

$$\tau_{ap} = \frac{1}{k_{tun,ap} + \gamma_{ap}} = \frac{1}{k_{ap} \exp(-\beta_{ap}(3.4(n + 1))) + \gamma_{ap}} \tag{20}$$

The rate γ_{ap} represents the competing recombination or relaxation rate.

By the application of our theory, we calculated $k_{ap} = 0.94$ ps^{-1} and $\beta_{ap} = 0.68$ $Å^{-1}$, and the competing recombination rate of AP* was found to be $\gamma_{ap} \approx 5.5 \times 10^{-3}$ ps^{-1}.

The comparison of theory and experiment in Figure 4 shows that the data fit for AP is consistent with our analysis of stilbene-capped hairpins. Furthermore, we were also able to use our model to predict charge transfer yields using eq 2. By applying our theoretically derived fit parameters, we were able to calculate CT yields $\Phi_0 = 0.945$, $\Phi_1 = 0.64$, $\Phi_2 = 0.15$, and $\Phi_3 = 0.016$ for $n = 0$, 1, 2, and 3, respectively. However, $\Phi_3 = 0.016$ is so small that it would be experimentally impossible to detect the difference in AP lifetime between $n = 2$ and $n = 3$ or a system with no G. This is evidenced by the error bars displayed for $n = 2$ and $n = 3$ (inset of Figure 4 in ref 12).

Unfortunately, the measurements of Wan et al. were not extended to longer AT bridges which would have given us the opportunity to verify their hypothesis that "[l]ong-range transport must occur on a longer time scale and with a different mechanism, possibly by hopping migration".[12]

An analysis of the nearest-neighbor CT rate k for systems consisting of a naphthaldiimide (NDI) electron acceptor and phenothiazine (PTZ) electron donor separated by $n = 4, ..., 8$ AT base pairs was performed by Takada et al.[14] Their data analysis yielded a substantially faster nearest-neighbor CT rate of $k = 20$ ns^{-1}.[14] We will show how we were able to construct a superior data fit for the systems studied by Takada et al.[14] consistent with the nearest-neighbor CT rate $k = 1.2$ ns^{-1}.

In ref 14, the nearest-neighbor CT rate for neighboring adenines was determined by fitting the data for the yield ratio Φ' to the kinetics model expression[14,33]

$$\Phi' = \frac{k_2/k_1}{1 + (N - 1)k_2/k} \tag{21}$$

where Takada et al. define $k_1 = 7.3 \times 10^{12}$ s^{-1} as the charge transfer rate from photoexcited NDI to the adjacent AT pair, $k_2 = 2.5 \times 10^{11}$ s^{-1} as the recombination transition of the positive charge from that AT pair back to NDI, and k as the nearest-neighbor CT rate between adjacent AT pairs. The values for k_1 and k_2 were taken from experimental data obtained for similar hairpins.[58]

Equation 21 is modeled after eq 3 in the work of Bixon et al.;[33] however, the $G^{+\bullet}$ deprotonation/water reaction rate k_r of Bixon et al.[33] is not applicable to the system of Takada et al., and the recombination rate k_1 is used instead. The rate $k_1 = 7.3 \times 10^{12}$ s^{-1} is indeed very large for NDI to AT CT because the driving force for this transition is determined to be 1 eV,[58] a value of ΔG in the inverted Marcus regime close to the optimal value for the fastest CT.

However, by setting $k_1 \approx k_2$ (as $k_0 \approx \gamma_2$ was determined to be for our system) and using the value $k \sim 2 \times 10^{10}$ s^{-1},[14] we were able to reproduce the data fit achieved by Takada et al. (the green line in Figure 5). After fitting the data points with a more general rational function of the form

$$\Phi' = \frac{A}{N + B} \tag{22}$$

we were able to achieve a near-perfect fit adjusting A and B so that

$$\Phi' = \frac{0.0423}{N - 2} \tag{23}$$

The behavior of eq 23 differs qualitatively from eq 21 and can be interpreted based on the specifics of charge transfer in $NDI(AT)_nPTZ$ hairpins. $\Phi' \propto 1/(N - 2)$ corresponds to the CT yield of the hairpin from the second A (second nearest A to NDI) to PTZ. If we take $k_2 \gg k$ and $K \gg k$, where K represents the CT rate from the last A to PTZ, and assuming that our model

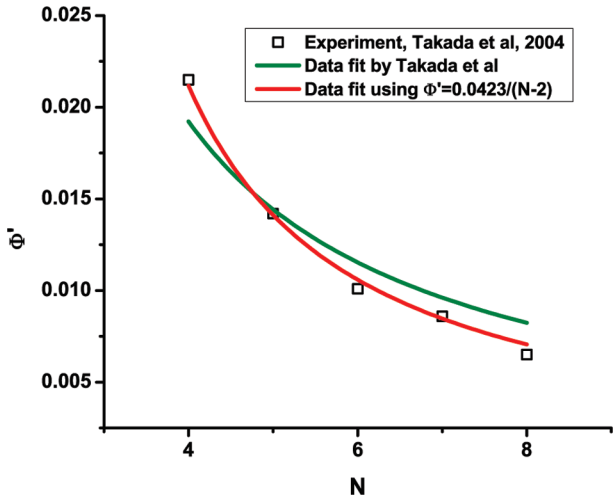

Figure 5. Dependence of CT yield ratio Φ' on the number N of AT base pairs. The green line and red line indicate the data fit using eq 21[14] and eq 23, respectively. The squares represent the experimentally derived data points.

is correct ($k \approx 1.2 \times 10^9$ s^{-1}), we indeed have $k/k_2 \approx 0.005$, indicating the charge on the first A inevitably recombines with NDI$^{-\bullet}$. Then the CT yield is determined by the ratio $1/(N-2)$ of path lengths (1 for the A adjacent to NDI and $N-2$ for the A adjacent to PTZ) to two "charge sinks". We suppose that the charge can tunnel directly from NDI to the second A with rate k_3 and that $k_3 \ll k_1$. Then the probability of this process is given by

$$P = \frac{k_3}{k_1} \tag{24}$$

If we assume that CT from NDI to PTZ is determined by this scenario, the CT yield can be expressed as

$$\Phi' = \frac{k_3/k_1}{N-2} \tag{25}$$

Equation 23 works well with the data of Takada et al. if $k_3 \approx 0.0423k_1$, in agreement with the standard CT rate decrease of an order of magnitude for each base pair in the bridge. We cannot provide analysis regarding relaxation times since yield data alone are insufficient. Time-resolved measurements are necessary to determine the charge hopping rate in DNA. We do not expect that hole tunneling from NDI to the second A is significant due to the small driving force for this process compared to the 1 eV driving force of CT from NDI to the nearest-neighboring A.[58]

V. Conclusion

We have performed a theoretical analysis on hole transfer kinetics and charge separation for stilbene-capped DNA hairpins of $n = 1, ..., 7$ identical AT pairs (Figure 1). Our model is based on experimental data from ref 10 and uses a simple Marcus theory model for charge hopping. For the rates shown in Figure 2, we found $k_{tun}(n) \approx 1.5 \times 8.3^{-n}$, $\gamma \approx 1.7 \times 10^{-3}$, $k_0 \approx 0.22 \times 10^{-3}$, $\gamma_1 \approx 0.29 \times 10^{-3}$, and $k \approx 1.2 \times 10^{-3}$ (all in inverse picoseconds). We have demonstrated that nearest-neighbor CT between adjacent AT pairs occurs slowly with an average time between hops on the order of 1.2 ns. This slow hopping rate can be understood in the context of adiabatic CT in a highly polar solvent with reorganization energy $\lambda \sim 0.83$ eV.

Our model shows that charge separation in stilbene-capped hairpins can occur by either direct charge tunneling or hopping over the $(AT)_n$ bridge after the formation of the [Sa$^{-\bullet}$A$^{+\bullet}$] exciplex within 30 ns of photoexcitation. For short bridge lengths $n < 4$, the positive charge tunnels from the exciplex directly to the stilbene donor group. For longer bridges ($n > 4$), charge transfer occurs mainly by hopping over the AT bridge. We suggest that charge hopping is not allowed until the Coulomb potential of the negatively charged stilbene acceptor group is screened by Na^+ counterion attachment. This conclusion agrees qualitatively with the work of Berashevich et al. and Voityuk et al. that was mainly focused on charge−solvent interaction.[15,18]

This hypothesis can be verified experimentally by substituting the Na^+ ion with another positive counterion. In particular, the binding of a large counterion such as NH_4^+ is much weaker and is therefore expected to slow down CT via the hopping channel. It would also be interesting to observe the outcome of replacing Na^+ with double charged ions like Ca^{2+} or Mg^{2+}. In fact, Ca^{2+} attachment to the Sa$^{-\bullet}$ group may even be more energetically favorable than for the Na^+ ion because of the double Coulomb attraction. Furthermore, after the attachment of a double charged ion, the hole may be biased toward charge separation resulting from Coulomb repulsion to the Ca^{2+}Sa$^{-\bullet}$ complex. This can make charge transfer much more efficient, and the charge separated state could exist for an extended period of time presenting new possibilities for DNA hairpins in solar energy applications.[10] It is possible that this complex may be more stable than Na^+Sa$^{-\bullet}$ because of the stronger Coulomb attraction and greater potential to form a covalent bond by the partial sharing of the extra electron associated with the Sa$^{-\bullet}$ radical. Experiments designed to test these predictions are planned.

Our kinetics model can be further tested by measuring the hole arrival time and the charge separation yield for longer AT bridges. For bridges of $n = 8$, 9, and 10 base pairs, we predict $\Phi_8 = 0.064$, $\tau_8 = 14$ ns; $\Phi_9 = 0.060$, $\tau_9 = 18$ ns; $\Phi_{10} = 0.056$, $\tau_{10} = 22$ ns (one should note that the deviation of our prediction for τ_{10} from the experimental result 13 ± 4 ns of Lewis et al.[64] can be due to the difficulty taking measurements at low yield and long times, $\tau_s > 10^4$ ps). These results were obtained by solving eq 1 with our previously determined optimum set of parameters: $k_{tun}(n) \approx 1.5 \times 8.3^{-n}$, $\gamma \approx 1.7 \times 10^{-3}$, $k_0 \approx 0.22 \times 10^{-3}$, $\gamma_1 \approx 0.29 \times 10^{-3}$, $k \approx 1.2 \times 10^{-3}$ (all in inverse picoseconds). One can see that the separation yield decreases very slowly with increasing bridge length, while hole arrival time at the Sd site notably increases in accordance with the diffusion law $\tau_n \propto n^2$. In the case of direct hole tunneling and in agreement with the recent results of Vura-Weis et al. for hole transport in diblock oligomers,[25] the arrival time is determined by $\tau = (k_{tun} + \gamma)^{-1}$ (see Figure 2) leading to a rapid decrease of time dependence on the bridge length (see Table 1). Consequently, in certain cases, the bridge length dependence of the charge travel time can be used to distinguish between hopping and tunneling mechanisms of charge transfer.

Experimental data for alternating AT sequences[64] can be qualitatively understood using a similar model that includes tunneling for shorter bridge lengths and hopping for longer bridge lengths. On the basis of yield behavior, one can estimate the hopping rate in alternating AT−TA base sequences to be about 5 times slower than that for the poly(A)−poly(T) systems studied in the present paper. This may be due to the longer

distance between diagonally situated adenines and the resulting larger solvent reorganization energy.[58,61]

We also applied our model to characterize the hole transfer between 2-aminopurine and guanine separated by a bridge of $n = 0$, 1, 2, and 3 AT pairs.[12] According to our analysis, CT in this system is associated with quantum tunneling. Our model CT rates fit the data within experimental accuracy and can predict n-dependent CT yields. In addition, we demonstrated that our kinetics model can be used to interpret the experimental data of Takada et al.[14] consistently with our slower nearest-neighbor CT rate $k = 1.2\ \mathrm{ns}^{-1}$. We believe that a time-resolved investigation of these and other systems will further confirm our predictions.

Our kinetics model analysis of CT in stilbene-capped hairpins demonstrates that the CT rate between adjacent AT pairs is relatively slow; one hopping event takes approximately 1 ns. We have similar expectations for GC pairs because CT is determined mostly by the reorganization energy (in the adiabatic regime) which is not critically dependent on the type of nucleobase. The slow nearest-neighbor CT rate of $1.2\ \mathrm{ns}^{-1}$ is a reasonable result since a CT rate an order of magnitude faster will critically increase irreversible UV damage to biological DNA found in living organisms. For this reason, biological DNA cannot behave as a molecular wire in its natural state. However, dry DNA is different and can have a fast enough CT rate that is potentially useful in molecular electronics.[6,8]

Acknowledgment. This work is supported by the NSF CRC Program, Grant Nos. 0628092 and 0628130, for AB and FDL, respectively. GSB acknowledges the support of the Department of Defense Science, Mathematics, and Research for Transformation Scholarship Program and the IBM Fellowship in Computational Science. The authors acknowledge Torsten Fiebig, Pierre Daublain, George Schatz, Mark Ratner, Mark Sulkes, and Larry Byers for productive discussions.

References and Notes

(1) Eley, D. D. *Research* **1959**, *12*, 293.
(2) Murphy, C. J.; Arkin, M. R.; Jenkins, Y.; Ghatlia, N. D.; Bossmann, S. H.; Turro, N. J.; Barton, J. K. *Science* **1993**, *262*, 1025.
(3) Genereux, J. C.; Barton, J. K. *Chem. Rev.* **2010**, *110*, 1642−1662.
(4) Rajski, S. R.; Jackson, B. A.; Barton, J. K. *Mutat. Res.* **2000**, *447*, 49.
(5) Genereux, J. C.; Boal, A. K.; Barton, J. K. *J. Am. Chem. Soc.* **2010**, *132*, 891–905. Shih, C. T.; Roche, S.; Romer, R. A *Phys. Rev. Lett.* **2008**, *1*, 018105.
(6) Porath, D.; Bezryadin, A.; de Vries, S.; Dekker, C. *Nature* **2000**, *403*, 635.
(7) Takada, T.; Kawai, K.; Fujitsuka, M.; Majima, T. *Proc. Natl. Acad. Sci.* **2004**, *101*, 14002.
(8) Xu, B. Q.; Zhang, P. M.; Li, X. L.; Tao, N. J. *Nano Lett.* **2004**, *4*, 1005.
(9) Mallajosyula, S. S.; Lin, J. C.; Cox, D. L.; Pati, S. K.; Singh, R. R. P. *Phys. Rev. Lett.* **2008**, *101*, 176805.
(10) Lewis, F. D.; Zhu, H.; Daublain, P.; Fiebig, T.; Raytchev, M.; Wang, Q.; Shafirovich, V. *J. Am. Chem. Soc.* **2006**, *128*, 791. Lewis, F. D.; Zhu, H. H.; Daublain, P.; Cohen, B.; Wasielewski, M. R. *Angew. Chem., Int. Ed.* **2006**, *45*, 7982–7985. Lewis, F. D.; Daublain, P.; Cohen, B.; Vura-Weis, J.; Shafirovich, V.; Wasielewski, M. R. *J. Am. Chem. Soc.* **2007**, *129*, 15130–15131.
(11) Wan, C.; Fiebig, T.; Kelley, S. O.; Treadway, C. R.; Barton, J. K.; Zewail, A. H. *Proc. Natl. Acad. Sci. U.S.A.* **1999**, *96*, 6014.
(12) Wan, C.; Fiebig, T.; Schiemann, O.; Barton, J. K.; Zewail, A. H. *Proc. Natl. Acad. Sci. U.S.A.* **2000**, *97*, 14052.
(13) Kawai, K.; Takada, T.; Tojo, S.; Majima, T. *J. Am. Chem. Soc.* **2003**, *125*, 6842.
(14) Takada, T.; Kawai, K.; Cai, X.; Sugimoto, A.; Fujitsuka, M.; Majima, T. *J. Am. Chem. Soc.* **2004**, *126*, 1125.
(15) Berashevich, J. A.; Chakraborty, T. *J. Phys. Chem. B* **2007**, *111*, 13465.
(16) Conwell, E. M.; Basko, D. M. *J. Am. Chem. Soc.* **2001**, *123*, 11441. Wang, X. F.; Chakraborty, T. *Phys. Rev. Lett.* **2006**, *97*, 106602.
(17) Conwell, E. M.; Bloch, S. M.; McLaughlin, P. M.; Basko, D. M. *J. Am. Chem. Soc.* **2007**, *129*, 9175.
(18) Voityuk, A. A.; Rösch, N.; Bixon, M.; Jortner, J. *J. Phys. Chem. B* **2000**, *104*, 9740.
(19) Siriwong, Kh.; Voityuk, A. A.; Newton, M. D.; Rösch, N. *J. Phys. Chem. B* **2003**, *107*, 14509.
(20) Voityuk, A. A. *J. Chem. Phys.* **2005**, *122*, 204904.
(21) Voityuk, A. A. *Chem. Phys. Lett.* **2008**, *451*, 153.
(22) Mantz, Y. A.; Gervasio, F. L.; Laino, T.; Parrinello, M. *Phys. Rev. Lett.* **2007**, *99*, 058104.
(23) Burin, A. L.; Uskov, D. B. *J. Chem. Phys.* **2008**, *129*, 025101.
(24) Grozema, F. C.; Tonzani, S.; Berlin, Y. A.; Schatz, G. C.; Siebbeles, L. D. A.; Ratner, M. A. *J. Am. Chem. Soc.* **2008**, *130*, 5157.
(25) Vura-Weis, J.; Wasielewski, M. R.; Thazhathveetil, A. K.; Lewis, F. D. *J. Am. Chem. Soc.* **2009**, *131*, 9722.
(26) Lewis, F. D.; Thazhathveetil, A. K.; Zeidan, T. A.; Vura-Weis, J.; Wasielewski, M. R. *J. Am. Chem. Soc.* **2010**, *132*, 444.
(27) Grozema, F. C.; Tonzani, S.; Berlin, Y. A.; Schatz, G. C.; Siebbeles, L. D. A.; Ratner, M. A. *J. Am. Chem. Soc.* **2009**, *131*, 14204.
(28) Kawai, K.; Kodera, H.; Osakada, Y.; Majima, T. *Nat. Chem.* **2009**, *1*, 156.
(29) Meggers, E.; Michel-Beyerle, M. E.; Giese, B. *J. Am. Chem. Soc.* **1998**, *120*, 12950.
(30) Henderson, P. T.; Jones, D.; Hampikian, G.; Kan, Y. Z.; Schuster, G. B. *Proc. Natl. Acad. Sci.* **1999**, *96*, 8353.
(31) Berlin, Y. A.; Burin, A. L.; Ratner, M. A. *J. Phys. Chem. A* **2000**, *104*, 443.
(32) Berlin, Y. A.; Burin, A. L.; Ratner, M. A. *J. Am. Chem. Soc.* **2001**, *123*, 260.
(33) Bixon, M.; Giese, B.; Wessely, S.; Langenbacher, T.; Michel-Beyerle, M. E.; Jortner, J. *Proc. Natl. Acad. Sci.* **1999**, *96*, 11713.
(34) Rips, I.; Jortner, J. *J. Chem. Phys.* **1987**, *87*, 2090.
(35) Lewis, F. D.; Zhu, H.; Daublain, P.; Sigmund, K.; Fiebig, T.; Raytchev, M.; Wang, Q.; Shafirovich, V. *Photochem. Photobiol. Sci.* **2008**, *7*, 534–539.
(36) Blaustein, G. S.; Demas, B.; Lewis, F. D.; Burin, A. L. *J. Am. Chem. Soc.* **2009**, *131*, 400.
(37) Lewis, F. D.; Liu, X.; Liu, J.; Miller, S. E.; Hayes, R. T.; Wasilewski, M. R. *Nature* **2000**, *406*, 51.
(38) Vura-Weis, J.; Wasielewski, M. R.; Thazhathveetil, A. K.; Lewis, F. D. *J. Am. Chem. Soc.* **2009**, *131*, 9722.
(39) Levich, V. G.; Dogonadze, R. R. *Dokl. Acad. Nauk SSSR* **1959**, *124*, 123.
(40) Ovchinnikov, A. A.; Ovchinnikova, M. Y. *Zh. Eksp. Teor. Fiziol.* **1969**, *56*, 1278.
(41) Zusman, L. D. *Chem. Phys.* **1980**, *49*, 295.
(42) Sparpaglione, M.; Mukamel, S. *J. Phys. Chem.* **1987**, *91*, 3938.
(43) Marcus, R. A. *J. Chem. Phys.* **1956**, *24*, 966.
(44) Marcus, R. A.; Sutin, N. *Biochim. Biophys. Acta* **1985**, *811*, 265.
(45) Marcus, R. A. *Rev. Mod. Phys.* **1993**, *65*, 599.
(46) Kubař, T.; Kleinekathöfer, U.; Elstner, M. *J. Phys. Chem. B* **2009**, *113*, 13107.
(47) Rösch, N.; Voityuk, A. A. *Top. Curr. Chem.* **2004**, *237*, 37.
(48) Steinbrecher, T.; Koslowski, T.; Case, D. A. *J. Phys. Chem. B* **2008**, *112*, 16935.
(49) Blancafort, L.; Voityuk, A. A. *J. Phys. Chem. A* **2006**, *110*, 6426.
(50) Sadowska-Aleksiejew, A.; Rak, J.; Voityuk, A. A. *Chem. Phys. Lett.* **2006**, *429*, 546.
(51) Kubař, T.; Woiczikowski, P. B.; Cuniberti, G.; Elstner, M. *J. Phys. Chem. B* **2008**, *112*, 7937.
(52) Mallajosyula, S. S.; Gupta, A.; Pati, S. K. *J. Phys. Chem. A* **2009**, *113*, 3955.
(53) Landau, L.; Lifshitz, E. *Quantum Mechanics: Non-Relativistic Theory*: Pergamon Press, 1977.
(54) Olofsson, J.; Larsson, S. *J. Phys. Chem. B* **2001**, *105*, 10398.
(55) Siriwong, Kh.; Voityuk, A. A.; Newton, M. D.; Rösch, N. *J. Phys. Chem. B* **2003**, *107*, 2595.
(56) Barnett, R. N.; Cleveland, C. L.; Joy, A.; Landman, U.; Schuster, G. B. *Science* **2001**, *294*, 567.
(57) Kubař, T.; Elstner, M. *J. Phys. Chem. B* **2008**, *112*, 8788.
(58) Lewis, F. D.; Kalgutkar, R. S.; Wu, Y.; Liu, X.; Liu, J.; Hayes, R. T.; Miller, S. E.; Wasilewski, M. R. *J. Am. Chem. Soc.* **2000**, *122*, 12346.
(59) Lewis, F. D.; Liu, J. Q.; Weigel, W.; Rettig, W.; Kurnikov, I. V.; Beratan, D. N. *Proc. Natl. Acad. Sci. U.S.A.* **2002**, *99*, 12536.
(60) Tong, G. S. M.; Kurnikov, I. V.; Beratan, D. N. *J. Phys. Chem. B* **2002**, *106*, 2381.
(61) Kubař, T.; Elstner, M. *J. Phys. Chem. B* **2009**, *113*, 5653.
(62) Khan, A. *J. Chem. Phys.* **2008**, *128*, 075101.
(63) Lewis, F.; Wu, T.; Zhang, Y.; Letsinger, R.; Greenfield, S.; Wasielewski, M. *Science* **1997**, *277*, 673.
(64) Lewis, F. D.; Daublain, P.; Cohen, B.; Vura-Weis, J.; Shafirovich, V.; Wasielewski, M. R. *J. Am. Chem. Soc.* **2007**, *129*, 15130.

JP101328T